Optimizing the Information Yield of 3-D OCT in Glaucoma

Springelkamp, Henriet; Lee, Kyungmoo; Ramdas, Wishal D.; Vingerling, Johannes R.; Hofman, Albert; Klaver, Caroline C. W.; Sonka, Milan; Abramoff, Michael D.; Jansonius, Nomdo M.

Published in:
Investigative ophthalmology & visual science

DOI:
10.1167/iovs.12-10551

Publication date:
2012

Optimizing the Information Yield of 3-D OCT in Glaucoma

Henriët Springelkamp,[1,2] *Kyungmoo Lee,*[3] *Wishal D. Ramdas,*[1,2] *Johannes R. Vingerling,*[1,2] *Albert Hofman,*[2] *Caroline C. W. Klaver,*[1,2] *Milan Sonka,*[3] *Michael D. Abràmoff,*[3–6] *and Nomdo M. Jansonius*[2,7]

Purpose. To determine, first, which regions of 3-D optical coherence tomography (OCT) volumes can be segmented completely in the majority of subjects and, second, the relationship between analyzed area and thickness measurement test–retest variability.

Methods. Three-dimensional OCT volumes (6 × 6 mm) centered around the fovea and optic nerve head (ONH) of 925 Rotterdam Study participants were analyzed; 44 participants were scanned twice. Volumes were segmented into 10 layers, and we determined the area where all layers could be identified in at least 95% (macula) or 90% (ONH) of subjects. Macular volumes were divided in 2 × 2, 4 × 4, 6 × 6, 8 × 8, or 68 blocks. We placed two circles around the ONH; the ONH had to fit into the smaller circle, and the larger circle had to fit into the segmentable part of the volume. The area between the circles was divided in 3 to 12 segments. We determined the test–retest variability (coefficient of repeatability) of the retinal nerve fiber layer (RNFL) and ganglion cell layer (RGCL) thickness measurements as a function of size of blocks/segments.

Results. Eighty-two percent of the macular volume could be segmented in at least 95% of subjects; for the ONH, this was 65% in at least 90%. The radii of the circles were 1.03 and 1.84 mm. Depending on the analyzed area, median test–retest variability ranged from 8% to 15% for macular RNFL, 11% to 22% for macular RGCL, 5% to 11% for the two together, and 18% to 22% for ONH RNFL.

Conclusions. Test–retest variability hampers a detailed analysis of 3-D OCT data. Combined macular RNFL and RGCL thickness averaged over larger areas had the best test–retest variability. (*Invest Ophthalmol Vis Sci.* 2012;53:8162–8171) DOI: 10.1167/iovs.12-10551

In open-angle glaucoma (OAG), damage to retinal ganglion cell axons results in visual field loss. Morphological signs of retinal cell damage and death are increased cupping of the optic nerve head (ONH), thinning of the retinal nerve fiber layer (RNFL),[1] and thinning of the retinal ganglion cell layer (RGCL).[2,3]

Morphological changes in OAG can be assessed qualitatively by fundoscopy and fundus photography. They can also be quantified with the Heidelberg Retina Tomograph (HRT; Heidelberg Engineering, Dossenheim, Germany)[4] and scanning laser polarimetry (GDx Nerve Fiber Analyzer; Carl Zeiss Meditec AG, Jena, Germany).[5,6] More recently, optical coherence tomography (OCT), and especially spectral-domain OCT,[7,8] have been added to this armamentarium. Unfortunately, the correspondence between imaging metrics and functional tests such as perimetry (the structure–function correlation) has been low to moderate.[9–13]

The information yield of 3-D OCT in glaucoma can, theoretically, be improved by quantitative analysis of the entire volume of tissues that are affected morphologically by OAG, the RNFL and the RGCL, over specific regions (regions of interest [ROI]) of these tissues. However, though analysis of increasingly smaller ROIs is attractive because it has the potential to better correlate with functional testing, the drawback is that test–retest variability may increase because fewer samples are available. The relationship between test–retest variability and ROI has been studied for peripapillary RNFL thickness measurements (see Discussion section). As far as we know, this relationship has not been studied for thickness measurements of macular RNFL or RGCL.

The aims of the present study were (1) to determine which regions of OCT volumes can be segmented accurately in the majority of subjects using the Iowa Reference Algorithm, which has been validated on the four most widely available commercial OCT scanners,[14–16] and (2) to unravel the relationship between ROI and test–retest variability.

Methods

Study Population and Data Collection

The Rotterdam Study is a prospective population-based cohort study investigating age-related disorders.[17] It is conducted in Ommoord, a

From the [1]Departments of Ophthalmology and [2]Epidemiology, Erasmus Medical Center, Rotterdam, The Netherlands; the Departments of [3]Electrical and Computer Engineering, [4]Ophthalmology and Visual Sciences, and [5]Biomedical Engineering, University of Iowa, Iowa City, Iowa; the [6]U.S. Department of Veterans Affairs, Iowa City, Iowa; and the [7]Department of Ophthalmology, University of Groningen, University Medical Center Groningen, Groningen, The Netherlands.

Presented at the annual meeting of The Netherlands Ophthalmological Society, Groningen, The Netherlands, March 2012, and the annual meeting of the Association for Research in Vision and Ophthalmology, Fort Lauderdale, Florida, May 2012.

Supported by Rotterdam: Stichting Lijf en Leven, Krimpen aan de Lek; MD Fonds, Utrecht; Rotterdamse Vereniging Blindenbelangen, Rotterdam; Stichting Oogfonds Nederland, Utrecht; Blindenpenning, Amsterdam; Blindenhulp, The Hague; Algemene Nederlandse Vereniging ter Voorkoming van Blindheid (ANVVB), Doorn; Landelijke Stichting voor Blinden en Slechtzienden, Utrecht; Swart van Essen, Rotterdam; Stichting Winckel-Sweep, Utrecht; Henkes Stichting, Rotterdam; Laméris Ootech BV, Nieuwegein; Medical Workshop, de Meern; Topcon Europe BV, Capelle aan de IJssel; all in The Netherlands; and Heidelberg Engineering, Dossenheim, Germany; Iowa: National Institute of Health Grant EY019112. The authors alone are responsible for the content and writing of the paper.

Submitted for publication July 9, 2012; revised October 23, 2012; accepted November 6, 2012.

Disclosure: **H. Springelkamp**, None; **K. Lee**, None; **W.D. Ramdas**, None; **J.R. Vingerling**, None; **A. Hofman**, None; **C.C.W. Klaver**, Rotterdam Study (S); **M. Sonka**, University of Iowa, P; **M.D. Abràmoff**, University of Iowa, P; **N.M. Jansonius**, None

Corresponding author: Michael D. Abràmoff, Department of Ophthalmology and Visual Sciences 11205 PFP, University of Iowa Hospitals and Clinics, Iowa City, IA 52242; michael-abramoff@uiowa.edu.

Investigative Ophthalmology & Visual Science, December 2012, Vol. 53, No. 13

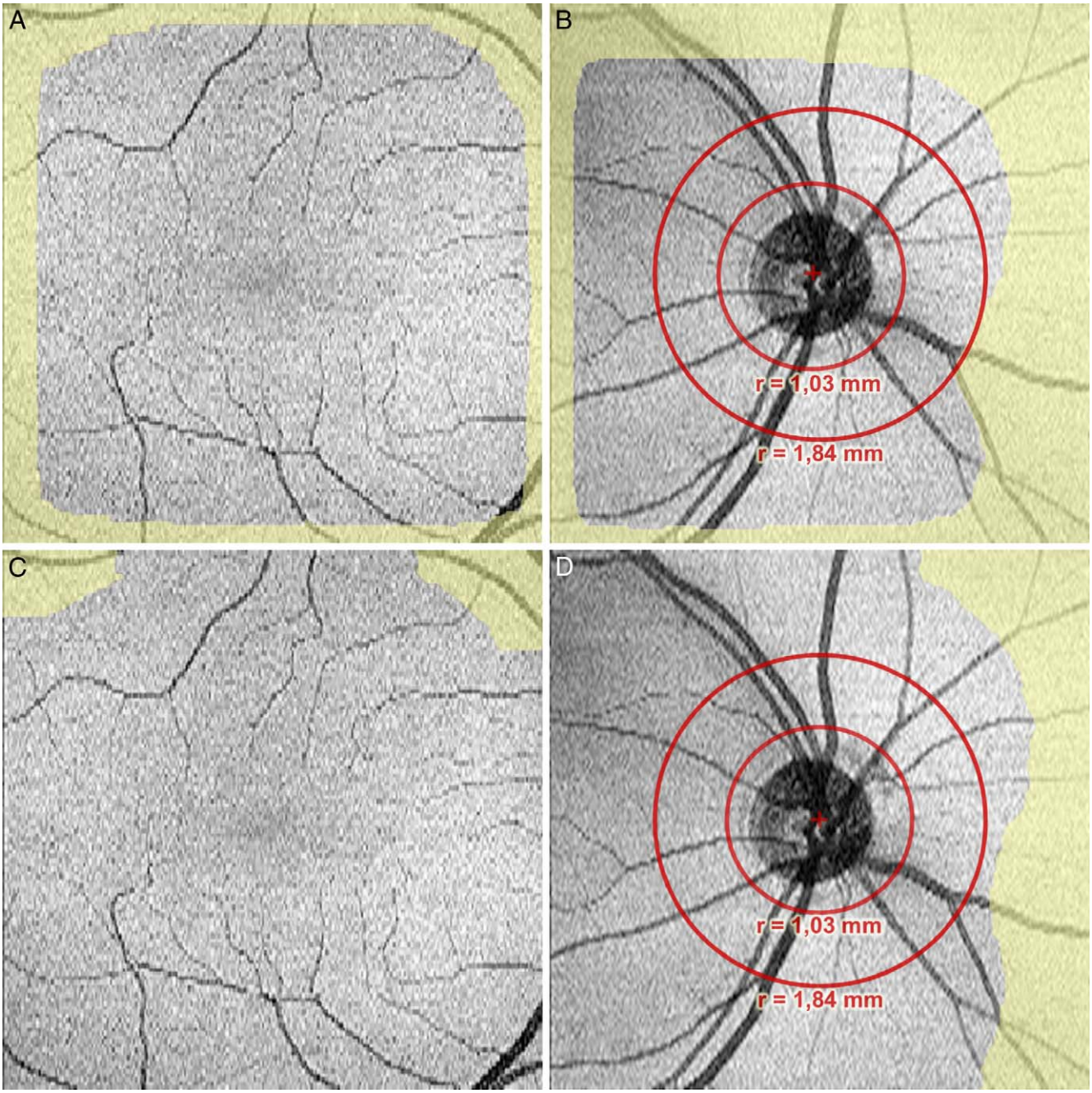

Figure 1. *Upper row* shows regions of the macular volume that are unsegmentable in ≥5% of subjects ([**A**], *yellow area*) and regions of the optic nerve head volume that are unsegmentable in ≥10% of subjects ([**B**], *yellow area*). *Inner circle* denotes area where ≥95% of optic nerve heads fit in if centered around the center of the optic nerve head (radius = 1.03 mm); *outer circle* is largest circle that fits in the *gray area* if centered around the center of the volume (radius = 1.84 mm). Right eye representation. *Lower row* (**C**, **D**) is similar to *upper row* (**A**, **B**), but now the volumes were not centered around the fovea/optic nerve head.

district of Rotterdam, The Netherlands. The study started in 1990 and is still ongoing. The original cohort comprised 7983 participants 55 years or older; ancillary studies were added later on, and in total 14,926 participants were enrolled. The ophthalmic examination as performed at baseline and at all follow-up examinations has been described before.[18] Measurements of intraocular pressure (IOP) and linear cup/disc ratio (LCDR), used for this paper, have also been described elsewhere.[19] In 2007, OCT scanning of the macular and ONH regions was added to the armamentarium.

All measurements were conducted after the Medical Ethics Committee of the Erasmus University had approved the study protocol and after all participants had provided written informed consent in accordance with the tenets of the Declaration of Helsinki.

OCT Data Collection

To determine which regions of the OCT volumes could be segmented in what fraction of subjects, the macula and ONH of 925 consecutive subjects was imaged with the Topcon 3-D OCT-1000 (Topcon, Tokyo,

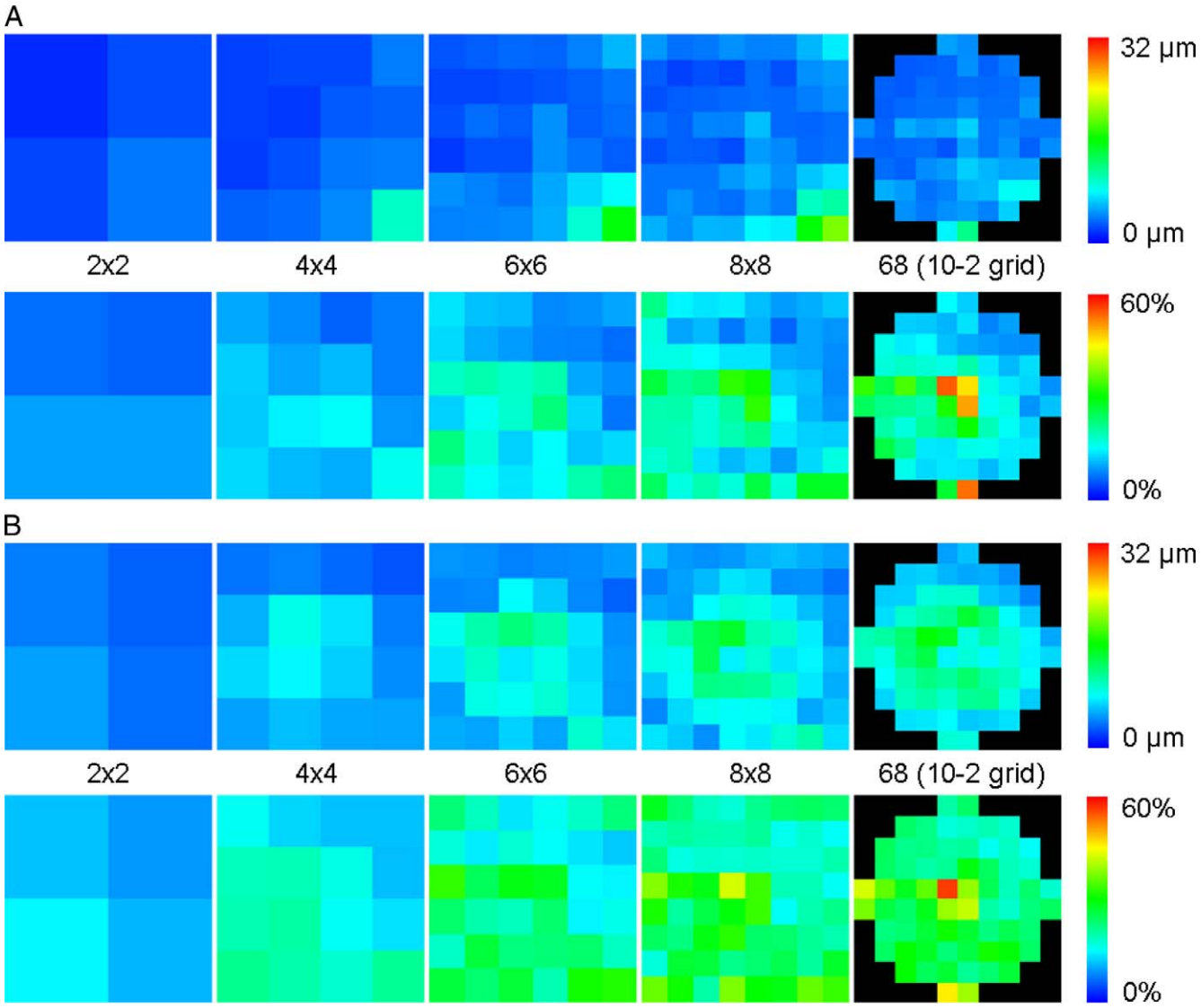

FIGURE 2. Test–retest variability (twice the standard deviation of the differences) for macular retinal nerve fiber layer (**A**) and macular retinal ganglion cell layer (**B**), both absolute (*upper row*, in micrometers) and relative to average thickness (*lower row*, in percentages).

Japan). Initially, both eyes were scanned; later, we confined the scanning to only the right eye because of time constraints in our population-based setting. Volume size was $6 \times 6 \times 1.68$ mm ($512 \times 128 \times 480$ voxels). Volumes were centered around the fovea and the ONH and performed in the horizontal direction. We excluded volumes with severe motion artifacts due to eye and head movements.

For the test–retest variability analysis, the macula and ONH of the right eye of 43 additional consecutive subjects and of the left eye of one subject were scanned twice on one day with the Topcon 3-D OCT-2000 (Topcon). Here, volume size was $6 \times 6 \times 2.30$ mm ($512 \times 128 \times 885$ voxels). In between the scans, the head was lifted from the chin rest. We excluded volumes with severe motion artifacts. Volumes with one or more blocks or segments (as defined below, Data Analysis, Test–Retest Variability subsection) where the RNFL or RGCL was completely unsegmentable were also excluded.

Data Analysis

Iowa Reference Algorithm, Segmentable Regions. Using our standard automated 3-D graph search approach,[14,20] all OCT volumes were segmented into 10 layers, demarcated by 11 surfaces. For each A-scan we determined, across subjects, the number of subjects for which all 10 layers could be defined, and then determined, after centering around the fovea and ONH, respectively, the largest continuous region where all layers could be defined in 95% of subjects for the macular region and in 90% of the subjects for the ONH region (see Discussion). Volumes of OS were flipped to get OD data format. A-scans that could be not segmented reliably by the algorithm were marked automatically.

Test–Retest Variability. We analyzed test–retest variability for a series of ROI grids. For the macula, the area of the volume was divided into 4 (2×2), 16 (4×4), 36 (6×6), 64 (8×8), and 68 (0.6×0.6 mm, following the 10–2 perimetry grid) square ROIs (blocks). For the ONH, we determined the radii of two circles. The radius of the larger circle was chosen so that it provides the largest circle that fit completely into the area that could be segmented in 90% of the subjects (see above) if centered on the x–y center of the volume. The radius of the smaller circle was chosen so that the ONH fit into the smaller circle completely in 95% of the subjects (peripapillary atrophy was allowed outside the smaller circle, as the RNFL can be segmented in areas with peripapillary atrophy). For the analyses, the circles were centered on the center of the individual ONH, and the area between the circles was divided into radially oriented ROIs (segments) of 120° (3 segments),

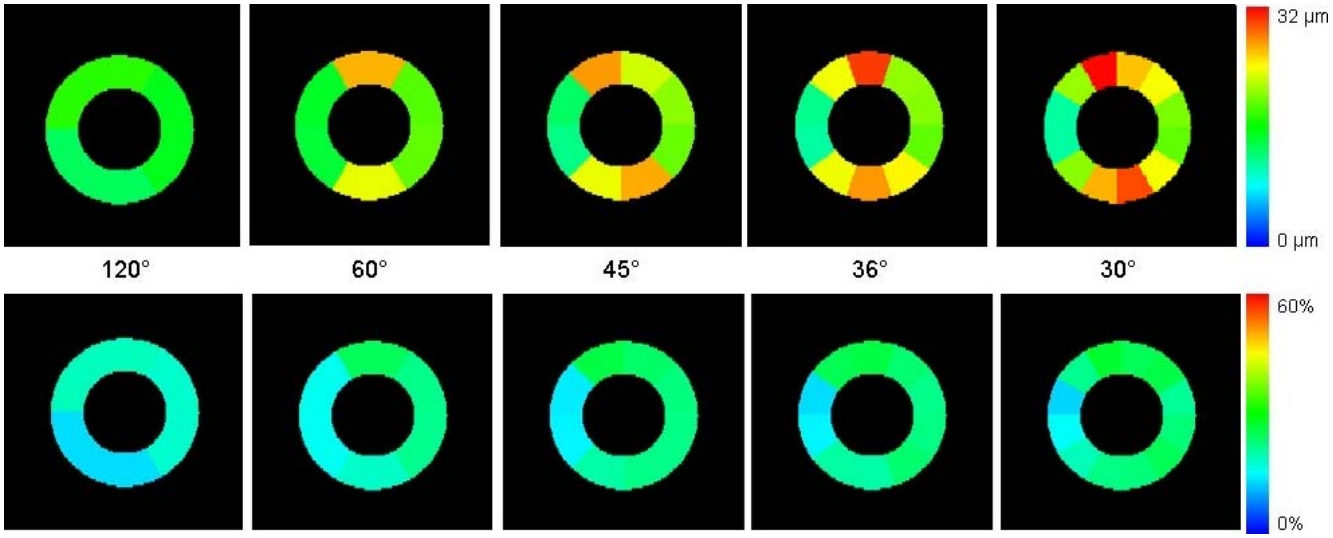

Figure 3. Test–retest variability (twice the standard deviation of the differences) for optic nerve head retinal nerve fiber layer; absolute (*upper row*, in micrometers) and relative to average thickness (*lower row*, in percentages).

60° (6 segments), 45° (8 segments), 36° (10 segments), and 30° (12 segments). We determined the position of the segments so that the raphe at the temporal side (assumed to be at the 9 o'clock position for the right eye) was always a demarcation between two segments. If a ROI was partially unsegmentable, the mean thickness of the RNFL or RGCL in the ROI concerned was based on the segmentable part. If one or more ROIs were completely unsegmentable, the volume was excluded (see above, OCT Data Collection subsection).

As a measure of test–retest variability, we used the coefficient of repeatability,[21] which is defined as two times the standard deviation of the signed differences between test and retest. Test–retest variability was determined for the thickness measurements of the ONH RNFL, macular RNFL, macular RGCL, and the sum of macular RNFL and RGCL. It was calculated both as absolute (in micrometers) and relative to average thickness (in percentages) for all ROIs. We used a general linear model to determine whether the test–retest variability was related to ROI size, mean thickness of the layer concerned, or location within the macular area. Here, the dependent variable was the unsigned relative difference between test and retest.

Normative Data. Normative data were based on the macular and ONH volumes of the right eyes of the 925 consecutive participants described above (OCT Data Collection subsection). We excluded participants with a positive family history of glaucoma, participants with an IOP above 21 mm Hg, and participants who received IOP-lowering treatment. We calculated the mean thicknesses with standard deviation and 95% central range (2.5th to 97.5th percentile) for the macular RNFL, macular RGCL, the sum of macular RNFL and RGCL, and the ONH RNFL.

All analyses were performed with IBM SPSS Statistics Release 19.0.0 (IBM Corp., Armonk, NY). A P value of 0.05 or less was considered statistically significant.

Results

For the segmentable region analysis, 976 macular volumes (897 OD; 79 OS) and 949 ONH volumes (874 OD; 75 OS) were available. The mean (standard deviation) age, IOP, and LCDR of these subjects were 57 (7) years, 14 (3) mm Hg, and 0.3 (0.2), respectively; 44% were male.

Figures 1A and 1B show the regions of the macular (Fig. 1A) and ONH (Fig. 1B) volumes that could be segmented in the majority of participants. Eighty-two percent of the area of the macular volume could be segmented in at least 95% of the subjects. Sixty-six percent of the area of the ONH volume could be segmented in at least 90% of the subjects. The radii of the inner and outer circles for the ONH volume were 1.03 and 1.84 mm, respectively (Fig. 1B). Figures 1C and 1D are similar to Figures 1A and 1B, but now the volumes were not centered around the fovea/ONH.

For the test–retest variability analysis, 30 pairs of macular volumes and 42 pairs of ONH volumes were available. Here, the mean (standard deviation) age, IOP, and LCDR were 71 (5) years, 14 (3) mm Hg, and 0.4 (0.2), respectively; 55% were male.

Figure 2 presents the absolute (in micrometers) and relative (in percentages) test–retest variability for the macular RNFL (Fig. 2A) and RGCL (Fig. 2B) thickness measurements per ROI for each grid. Figure 3 shows the test–retest variability for the ONH RNFL thickness measurements per ROI for each grid. Figure 4 gives the median, minimum, and maximum test–retest variability for each grid for the macular RNFL (Fig. 4A), the macular RGCL (Fig. 4B), the macular RNFL and RGCL combined (Fig. 4C), and the ONH RNFL (Fig. 4D). Test–retest variability increased with a more detailed grid. For the individual macula layers, only the 2×2 and 4×4 (RNFL) grids achieved a median test–retest variability of 10% or better. When we combined the two macula layers, the test–retest variability decreased substantially: For the combined layers, the median test–retest variability of the thickness measurements ranged from 5% (2×2 grid) to 11% (8×8 grid). For the ONH, the test–retest variability was <20% only for the 120° and 60° grids. The test–retest variability depended significantly on the ROI size ($P < 0.001$ for macular RNFL, RGCL, and the two combined; $P = 0.02$ for ONH RNFL); the mean thickness of the layer concerned ($P < 0.001$ for macular RNFL; $P = 0.002$ for macular RGCL; $P < 0.001$ for macular RNFL and RGCL combined; and $P < 0.001$ for ONH RNFL); and location within the macular area ($P < 0.001$).

Figure 5 shows the mean thicknesses for the macular RNFL (Fig. 5A) and macular RGCL (Fig. 5B) as a function of grid size. Figure 6 presents the mean thicknesses for the ONH RNFL. Table 1 presents the descriptive statistics of the normative data for the 2×2 macular grid and the 120° ONH segments. These data were based on 795 macular volumes and 781 ONH volumes.

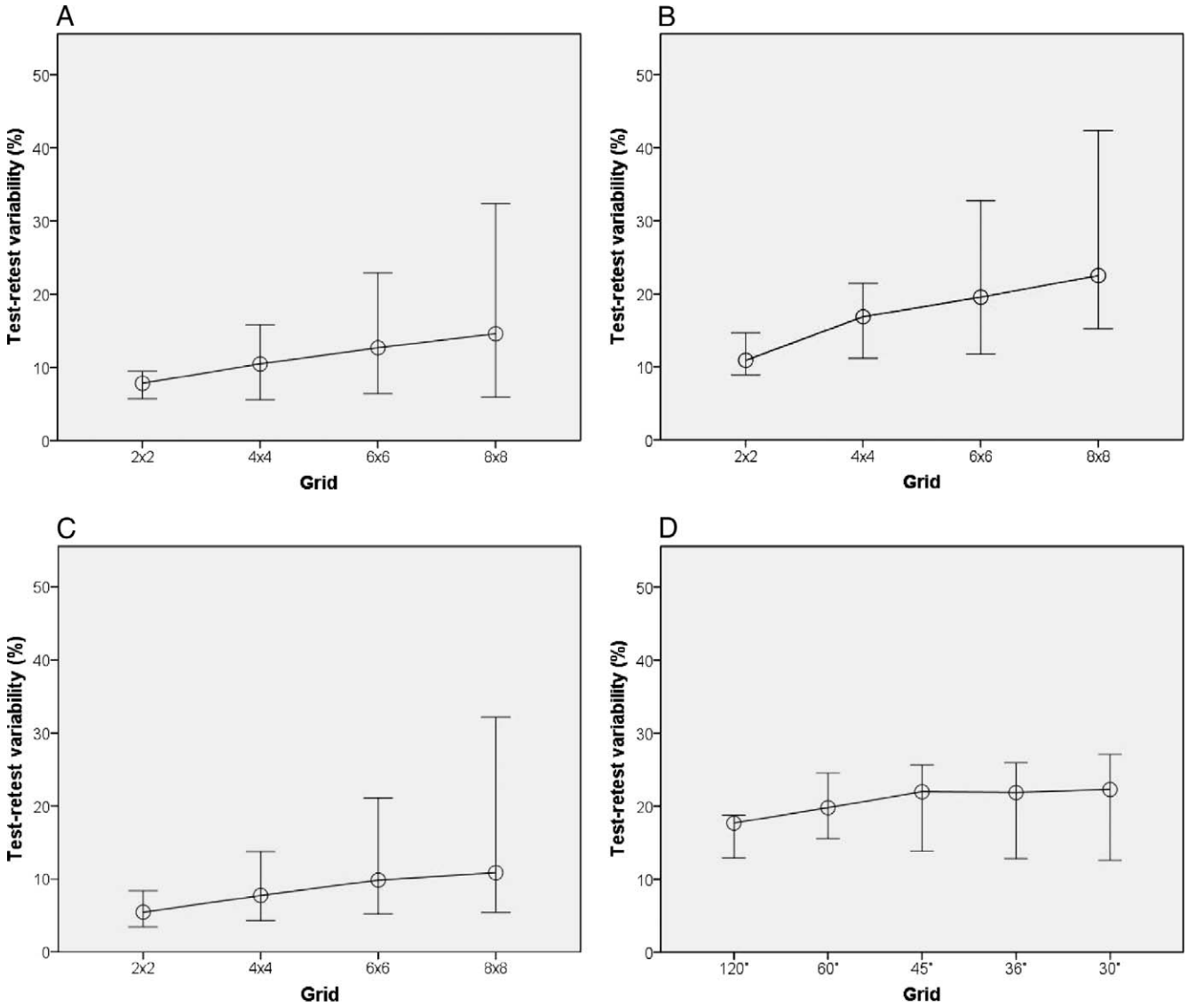

Figure 4. Test–retest variability of the thickness measurements presented as median with minimum and maximum of the various grids as displayed in Figures 2 and 3. (**A**) Macular retinal nerve fiber layer (RNFL); (**B**) macular retinal ganglion cell layer (RGCL); (**C**) macular RNFL and RGCL combined; (**D**) optic nerve head (ONH) retinal nerve fiber layer.

Discussion

The results of this study show that essentially the entire volume of the macula could be segmented and that test–retest variability depends on the size of the ROI. Unsegmentable regions were more common around the ONH, especially on the nasal side. We achieved the best test–retest variability for the combined RNFL/RGCL thickness measurements in the macular area.

The area of the macular volume that was segmentable in at least 95% of the subjects (Fig. 1A) was initially determined after centering on the fovea. The rationale of this centering is to compare corresponding regions of the retina between subjects. Figure 1A shows a clear vignetting. This might be caused either by poor volume quality toward the borders of the volume or by poor centering during the scanning process. Figure 1C shows the same analysis as Figure 1A but now without centering on the fovea. In this analysis, 96% of the area of the macular volume could be segmented in at least 95% of the subjects (to be compared to 82% in Fig. 1A). Hence, the volume quality does not diminish toward the borders of the volume (except for the two small regions in the upper corners). Rather, centering during the imaging process was suboptimal in our study.

Because many ONH volumes had a large unsegmentable region at the nasal side, we arbitrarily adopted a 90% threshold for determining the segmentable part of the ONH volume. If we had used a 95% threshold for ONH, it would have been possible to segment only 54% of the volume (to be compared to 66% for the 90% threshold). Again, some vignetting can be seen, which disappeared largely after the removal of centering on the ONH during the data analysis process (Fig. 1D). In Figure 1D, 84% of the area of the ONH volume could be segmented in at least 90% of the subjects (to be compared to 66% in Fig. 1B). The unsegmentable region at the nasal side, however, remained clearly visible, indicating that volume quality is a real issue in this region. Due to imperfect centering during the scanning process, the actual percentage of rings with unsegmentable regions was 12.5% rather than 10%; but in only 4.8%, the unsegmentable part continued up to the inner circle, making it impossible to determine RNFL thickness in

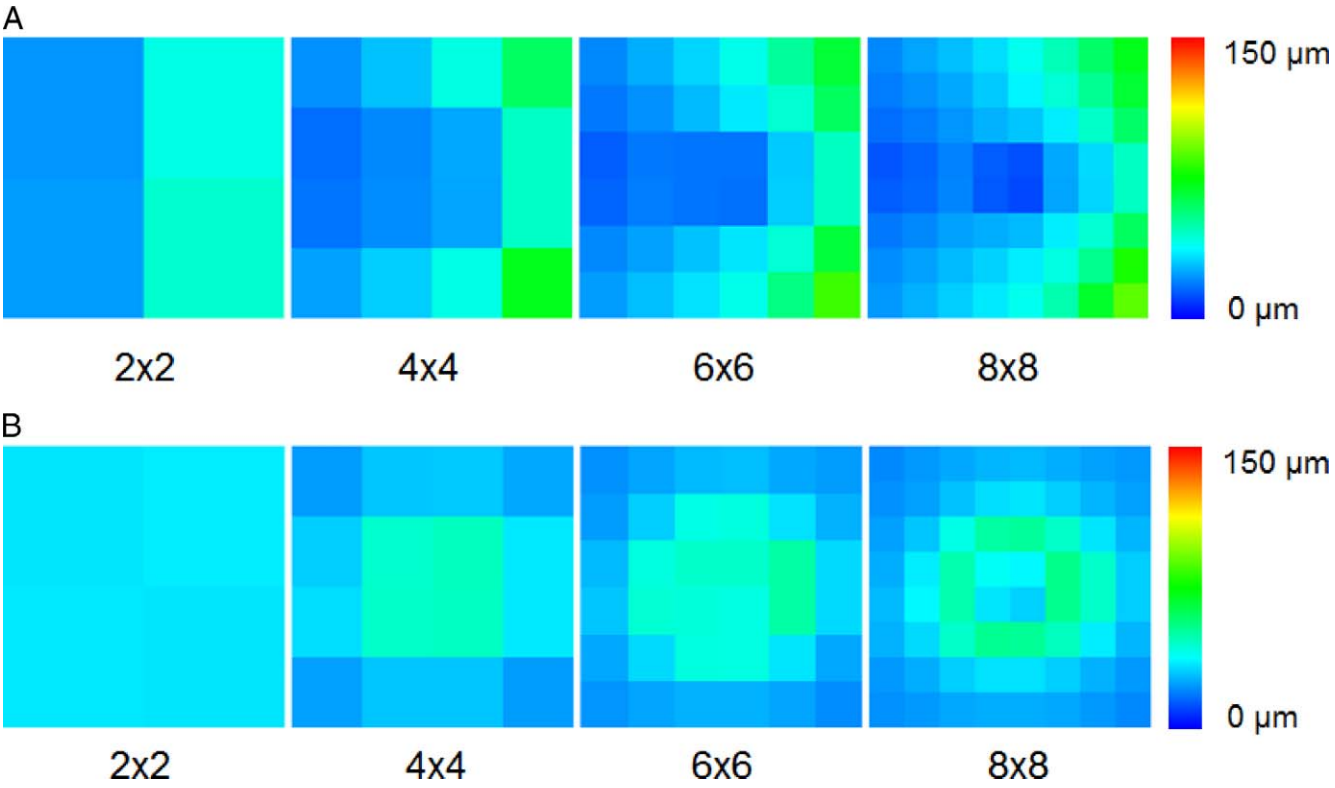

Figure 5. Normative data (*color graphs* for all grids except the 10–2 grid, in micrometers) for macular retinal nerve fiber layer (**A**) and macular retinal ganglion cell layer (**B**).

part of the circumference. In the remaining 7.7%, the thickness determination was based on the part that was still segmentable. In 80% of the 12.5% with unsegmentable regions within the ring, the unsegmentable regions were located at the nasal side of the ONH.

A possible explanation for the finding that unsegmentable regions were more common in the ONH volumes than in the macular volumes is the fact that the ONH volume has a greater distance to the optical axis of the eye.[22] The observed higher frequency of unsegmentable regions at the nasal side of the ONH is in line with this explanation. The segmentable area could also be influenced by image quality. Unfortunately, the OCT device used in our study does not provide an image quality parameter. As a proxy, we averaged the signal strength, per subject, over all voxels and plotted the resulting value as a function of the area that could be segmented. Figure 7 shows the results for the macular area (Fig. 7A) and ONH (Fig. 7B). As can be seen in these figures, there is possibly some but no clear relationship between mean signal strength and segmentable area.

For the coarsest grid (2 × 2 ROIs) of the macular volume, we reached a test–retest variability of 6% to 9% for the RNFL, with the highest values located inferiorly. With more detailed grids, the inferior region and especially the foveal area had the highest test–retest variability. These areas also showed the highest test–retest variability for the RGCL. To our knowledge, only DeBuc et al.[23] have examined the test–retest variability for RNFL in a 6 × 6 mm macular volume. They found a coefficient of repeatability of 4.6% for the mean RNFL thickness. Mean RNFL thickness test–retest variability for the macular volume as a whole was 4.0% in our data, in good agreement with DeBuc et al. Other studies addressing test–retest variability of OCT thickness measurements focused on the thickness of the entire retina in circular (EDTRS) grids. Neither of these is useful from the point of view of glaucoma.

Table 2 summarizes studies that reported on test–retest variability of peripapillary RNFL thickness measurements. Some of these studies measured at different segment sizes and showed that test–retest variability increased with an increasing number of segments. Test–retest variability was generally highest superiorly (11 to 1 o'clock position) and

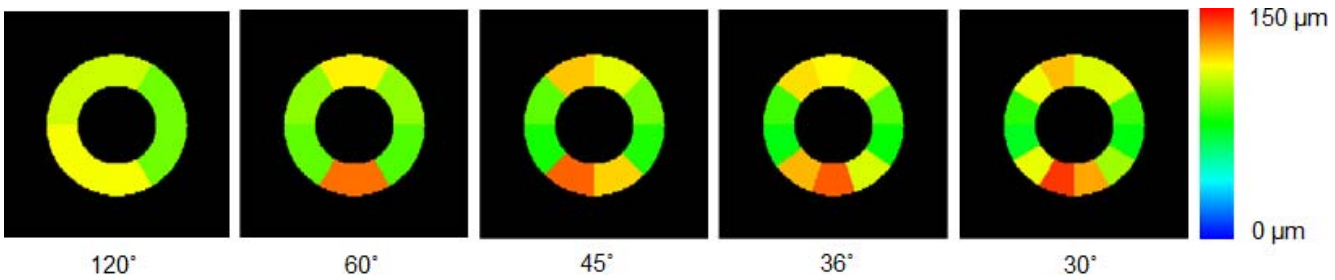

Figure 6. Normative data (*color graphs* for all grids, in micrometers) for optic nerve head retinal nerve fiber layer.

Table 1. Normative Data for RNFL Thickness, RGCL Thickness, and the Combined Layers for the 2 × 2 Block Grid in the Macular Region and for the RNFL Thickness for the 120° Segments in ONH Region

	Mean Thickness, μm (Standard Deviation; 95% Central Range)
Macular RNFL	
Temporal superior	22 (3; 17–27)
Nasal superior	41 (7; 28–54)
Temporal inferior	23 (3; 18–30)
Nasal inferior	44 (8; 29–61)
Macular RGCL	
Temporal superior	34 (5; 24–43)
Nasal superior	35 (4; 27–43)
Temporal inferior	34 (4; 25–43)
Nasal inferior	34 (4; 25–41)
Macular RNFL + RGCL	
Temporal superior	56 (6; 43–67)
Nasal superior	76 (9; 58–92)
Temporal inferior	58 (6; 45–69)
Nasal inferior	78 (10; 58–95)
ONH RNFL	
Temporal superior	105 (18; 55–135)
Nasal	92 (19; 49–129)
Temporal inferior	112 (17; 65–139)

inferiorly (5 to 6 o'clock position)—the areas where the major vessels can be found. This is in agreement with our data (Fig. 3). Different definitions of test–retest variability have been used in the literature (Table 2). Only studies applying the same definition should be compared. Since we did not look at the quarter grid, we can compare the test–retest variability for only the clock hour grid. Budenz et al.[24] showed a median test–retest variability of 14.3 μm in 51 glaucoma patients. In normal eyes, a median test–retest variability of 16.3 μm[25] and 15.9 μm[26] was reported (converted to our definition). Our median test–retest variability of 22.3 μm is somewhat higher. In our study, the two volumes were recorded and analyzed independently; they were not superimposed and aligned before analysis, nor was an eye-tracking system used. For follow-up of a single patient, such measures could lower test–retest variability and thus improve change detection. With our approach, however, the test–retest variability gives a more realistic estimate of the accuracy of single scans, which are often used in screening settings and in population-based studies. A lower test–retest variability after registration of a previous scan was found in the study of Kim et al.[26] In that study, median test–retest variability decreased after application of two different registration methods (from 8.2 to 6.3 and 6.8 μm, respectively).

A strength of this study is the sample size. Segmentable regions and normative data were based on almost a thousand subjects. The population-based setting and the fact that we used volumes of consecutive participants should have made our sample as unbiased as possible. OAG cases previously identified within the study were excluded, as were participants with an increased OAG risk (see Methods section). Together with the low prevalence of OAG in the general population, this should ensure an appropriate dataset for determining normative data.

A limitation of this study is the quality of the scans. Due to limited time for scanning, centering of the fovea and ONH was suboptimal, and scans with motion artifacts could not be repeated. Scans performed in a clinical setting (as opposed to our population-based setting) could have larger segmentable areas. This remains to be proven, though. Another drawback is the use of two different OCT devices (Topcon 3-D OCT-1000 and OCT-2000; Topcon) with different volume sizes, due to an update during the course of the study. Within the substudies (segmentable regions and test–retest variability), however, we used the same OCT device for all participants. The older age of the participants in our two substudies (71 and 57 years, respectively) may have made it more difficult to get high-quality scans, due to a higher frequency of ocular morbidity such as cataract. On the other hand, OAG also typically occurs in the elderly, and our scan quality would therefore be representative for the target population.

In the macular volume, a combined thickness measurement of the two layers studied (RNFL and RGCL) improved the repeatability significantly. This indicates that the border between the RNFL and RGCL has a relatively large variability on repeat scanning. However, a good repeatability alone is not sufficient to obtain a good diagnostic performance. Focusing on tissues relevant to the disease of interest is also important.

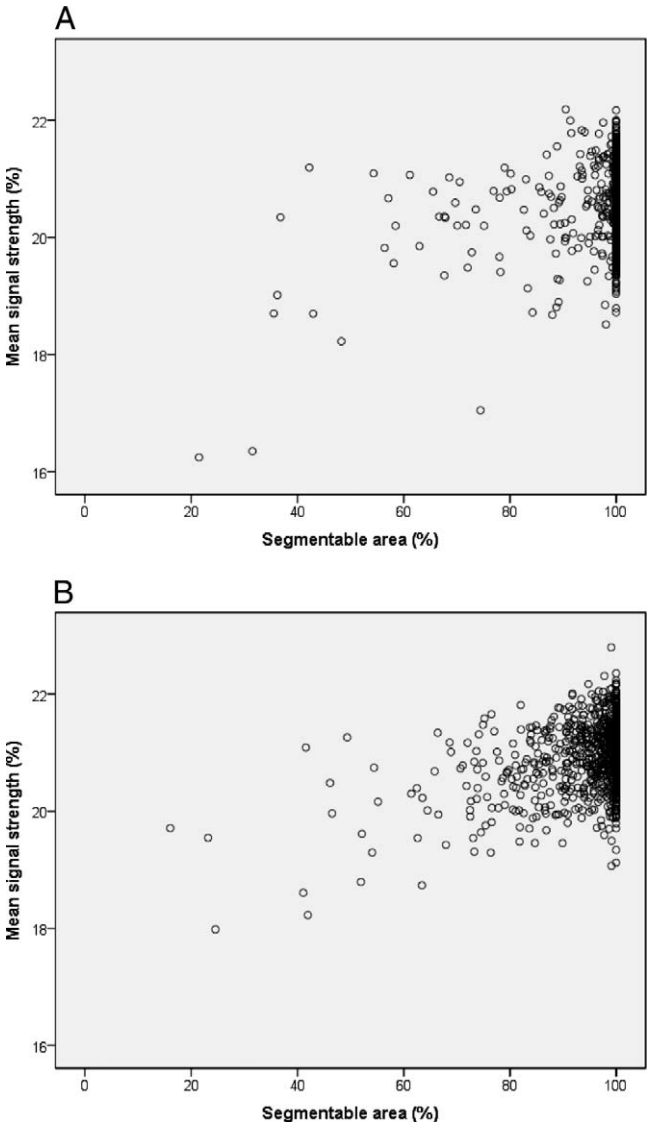

Figure 7. Mean signal strength (percentage of maximum) as a function of segmentable area (percentage of maximum) for the macular area (**A**) and ONH (**B**).

Table 2. Literature Overview of Test–Retest Variability for Peripapillary Retinal Nerve Fiber Layer Measurements

Author	Study Population	Mean Age, y	Definition TRV	Median TRV, μm (Range), Quarter Grid	Median TRV, μm (Range), Clock Hour Grid	Region(s) with Worst TRV
Budenz (2008)[24]	Glaucoma ($n = 51$)	69.5	2 × square root of within-day variance components	10 (6.2–12.5)	14.3 (9.3–17.1)	6 and 12 o'clock
Kim (2011)[27]	Normal ($n = 359$) and glaucoma ($n = 263$)	49.8 (all)	2 × square root of the variance between two repeated measurements	6.3 (5.8–7.8)	NA	Inferior quadrant
Garas (2010)[28]	Normal and ocular hypertensive ($n = 14$) and glaucoma ($n = 23$)	56.7 (normal and hypertensive) and 58.3 (glaucoma)	1.96 × intrasession SD	7.1 (6.5–8.7) (all)	NA	Superior quadrant
Carpineto (2012)[25]	Normal ($n = 68$)	29.1	1.96 × SD of differences between measurements	12.9 (7.8–17.0)	16.0 (9.6–30.4)	6 and 12 o'clock
Kim (2009)[26]	Normal (14 subjects, 27 eyes)	37.3	SD (approximately the average of all eyes)	8.2 (4.5–9.0), 6.3 (2.2–9.5), 6.8 (2.6–8.8)*	8.0 (3.6–13.6)	5 and 11 o'clock
Paunescu (2004)[29]	Normal ($n = 10$)	30.5	Intravisit SD (within subject, within date)	2.3 (2.0–3.4)	3.1 (1.5–5.3)	6 and 11 o'clock
Mwanza (2010)[30]	Glaucoma ($n = 55$)	70.7	Pooled within-subject test–retest SD (3 measurements)	2.5 (2.2–2.8)	3.6 (2.2–4.5)	3, 6, and 11 o'clock
Budenz (2005)[31]	Normal ($n = 88$) and glaucoma ($n = 59$)	53 (normal) and 68 (glaucoma)	2 × SD of three repeated measurements	9.7 (7.5–10.2) (normal) and 10.4 (5.6–10.7) (glaucoma)	NA	Nasal quadrant (normal) and superior (glaucoma)
Hong (2010)[32]	Normal ($n = 36$ eyes of 30 subjects)	28.6	2 × square root of the variance among three repeated measurements	7.5 (5.8–8.1)	10.0 (4.7–13.6)	2 and 6 o'clock
Lee (2010)[33]	Normal ($n = 98$) and glaucoma ($n = 79$)	51.1 (normal) and 58.7 (glaucoma)	2 × SD of each set of three repeated measurements	7.5 (5.6–8.3) (normal) and 6.7 (4.6–7.2) (glaucoma)	9.5 (7.3–11.5) (normal) and 8.8 (5.0–10.0)	6 and 11 o'clock (normal) and 1 and 5 o'clock (glaucoma)
Savini (2010)[34]	Normal ($n = 32$)	59	2 × SD of three repeated measurements	4.4 (2.6–5.6)	7.3 (2.7–9.3)	6 and 12 o'clock
Mansoori (2011)[35]	Normal ($n = 61$) and glaucoma ($n = 41$)	38.3 (normal) and 57.2 (glaucoma)	2 × SD of three repeated measurements	2.5 (1.9–3.0) (normal) and 2.4 (1.9–2.9) (glaucoma)	NA	Superior (normal) and nasal (glaucoma)
Nakatani (2011)[36]	Normal ($n = 32$) and glaucoma ($n = 32$)	57.3 (normal) and 61.5 (glaucoma)	2 × mean within-participant SD of three repeated measurements	11.7 (10.3–14.0) (normal) and 10.7 (8.7–14.7) (glaucoma)	15.3 (12.8–18.0) (normal) and 13.3 (10.1–18.9) (glaucoma)	8 o'clock (normal) and 4 o'clock (glaucoma)
Leung (2009)[37]	Normal ($n = 16$)	52	2.77 × intravisit within-subject SD	8.0 (6.8–9.7)	12.2 (7.5–15.0)	6 and 11 o'clock
Hong (2012)[38]	Normal ($n = 75$)	43.7	2.77 × within-subject SD	11.2 (5.4–12.5)	NA	Nasal quadrant
Tan (2012)[39]	Normal ($n = 50$)	35.6	2.77 × within-subject SD	8.5 (7.1–11.3) (Cirrus) and 7.8 (6.3–9.1) (Spectralis)	NA	Superior (Cirrus) and temporal (Spectralis)

TRV, test–retest variability; SD, standard deviation.

* First TRV is TRV without eye tracking; second and third TRV are TRV with different methods of eye tracking.

As both the RNFL and the RGCL are involved in OAG, a combined analysis of these two layers seems, a priori, a logical approach. In order to get a first impression of the diagnostic performance (which will be addressed in detail in a further study), we calculated areas under the receiver operating characteristic curves (AUCs) for the average thicknesses of the macular RNFL, the macular RGCL, and both layers together. We found AUCs of 0.89, 0.87, and 0.92, respectively, based on the participants used in this study as controls and 21 eyes of 21 OAG patients as cases. These 21 OAG cases were a random subset of OAG cases identified previously in the Rotterdam Study who had had an OCT scan.[18,40] The average (range) standard automated perimetry mean deviation was −9.1 dB (−1.4 to −21.8 dB). Although the differences between these AUCs were—possibly related to the small number of OAG cases—not statistically significant, the point estimates indicate that a thorough study of the combined analysis of the two layers is worth the effort.

In conclusion, it is possible to obtain detailed thickness measurements, but there is a balance between the ROI size and variability. In the macular volume, a combined thickness measurement of the two layers studied (RNFL and RGCL) improved the repeatability significantly. The optimal grid size for screening and progression detection in glaucoma can be deduced by comparing cross-sectional measurements in healthy subjects and glaucoma patients and by performing longitudinal measurements in glaucoma patients, respectively. These issues, including a confirmation of the presumed superiority of a combined analysis of the RNFL and RGCL, should all be addressed before OCT scanning can be optimally used in clinical practice.

References

1. Airaksinen PJ, Alanko HI. Effect of retinal nerve fibre loss on the optic nerve head configuration in early glaucoma. *Graefes Arch Clin Exp Ophthalmol*. 1983;220:193–196.
2. Quigley HA. Open-angle glaucoma. *N Engl J Med*. 1993;328: 1097–1106.
3. Nickells RW. Ganglion cell death in glaucoma: from mice to men. *Vet Ophthalmol*. 2007;10(suppl 1):88–94.
4. Rohrschneider K, Burk RO, Kruse FE, et al. Reproducibility of the optic nerve head topography with a new laser tomographic scanning device. *Ophthalmology*. 1994;101:1044–1049.
5. Weinreb RN, Dreher AW, Coleman A, et al. Histopathologic validation of Fourier-ellipsometry measurements of retinal nerve fiber layer thickness. *Arch Ophthalmol*. 1990;108:557–560.
6. Dreher AW, Reiter K. Retinal laser ellipsometry: a new method for measuring the retinal nerve fibre layer thickness distribution? *Clin Vis Sci*. 1992;7:481–488.
7. Hee MR, Puliafito CA, Wong C, et al. Optical coherence tomography of macular holes. *Ophthalmology*. 1995;102:748–756.
8. Schuman JS, Hee MR, Arya AV, et al. Optical coherence tomography: a new tool for glaucoma diagnosis. *Curr Opin Ophthalmol*. 1995;6:89–95.
9. Hood DC, Anderson SC, Wall M, et al. Structure versus function in glaucoma: an application of a linear model. *Invest Ophthalmol Vis Sci*. 2007;48:3662–3668.
10. Lee JR, Jeoung JW, Choi J, et al. Structure-function relationships in normal and glaucomatous eyes determined by time- and spectral-domain optical coherence tomography. *Invest Ophthalmol Vis Sci*. 2010;51:6424–6430.
11. Hood DC, Raza AS. Method for comparing visual field defects to local RNFL and RGC damage seen on frequency domain OCT in patients with glaucoma. *Biomed Opt Express*. 2011;2: 1097–1105.
12. Rao HL, Zangwill LM, Weinreb RN, et al. Structure-function relationship in glaucoma using spectral-domain optical coherence tomography. *Arch Ophthalmol*. 2011;129:864–871.
13. Garvin MK, Abramoff MD, Lee K, et al. 2-D pattern of nerve fiber bundles in glaucoma emerging from spectral-domain optical coherence tomography. *Invest Ophthalmol Vis Sci*. 2012;53:483–489.
14. Garvin MK, Abramoff MD, Wu X, et al. Automated 3-D intraretinal layer segmentation of macular spectral-domain optical coherence tomography images. *IEEE Trans Med Imaging*. 2009;28:1436–1447.
15. Lee K, Niemeijer M, Garvin MK, et al. Segmentation of the optic disc in 3-D OCT scans of the optic nerve head. *IEEE Trans Med Imaging*. 2010;29:159–168.
16. Abramoff MD, Lee K, Niemeijer M, et al. Automated segmentation of the cup and rim from spectral domain OCT of the optic nerve head. *Invest Ophthalmol Vis Sci*. 2009;50: 5778–5784.
17. Hofman A, Duijn van CM, Franco OH, et al. The Rotterdam Study: 2012 objectives and design update. *Eur J Epidemiol*. 2011;26:657–686.
18. Wolfs RC, Borger PH, Ramrattan RS, et al. Changing views on open-angle glaucoma: definitions and prevalences–The Rotterdam Study. *Invest Ophthalmol Vis Sci*. 2000;41:3309–3321.
19. Ramdas WD, Wolfs RC, Hofman A, et al. Heidelberg Retina Tomograph (HRT3) in population-based epidemiology: normative values and criteria for glaucomatous optic neuropathy. *Ophthalmic Epidemiol*. 2011;18:198–210.
20. Quellec G, Lee K, Dolejsi M, et al. Three-dimensional analysis of retinal layer texture: identification of fluid-filled regions in SD-OCT of the macula. *IEEE Trans Med Imaging*. 2010;29: 1321–1330.
21. Altman DG. *Practical Statistics for Medical Research*. London: Chapman & Hall; 1991.
22. Gao W, Cense B, Zhang Y, et al. Measuring retinal contributions to the optical Stiles-Crawford effect with optical coherence tomography. *Opt Express*. 2008;16:6486–6501.
23. DeBuc DC, Somfai GM, Ranganathan S, et al. Reliability and reproducibility of macular segmentation using a custom-built optical coherence tomography retinal image analysis software. *J Biomed Opt*. 2009;14:064023.
24. Budenz DL, Fredette MJ, Feuer WJ, et al. Reproducibility of peripapillary retinal nerve fiber thickness measurements with stratus OCT in glaucomatous eyes. *Ophthalmology*. 2008;115: 661–666, e4.
25. Carpineto P, Nubile M, Agnifili L, et al. Reproducibility and repeatability of Cirrus HD-OCT peripapillary retinal nerve fibre layer thickness measurements in young normal subjects. *Ophthalmologica*. 2012;227:139–145.
26. Kim JS, Ishikawa H, Sung KR, et al. Retinal nerve fibre layer thickness measurement reproducibility improved with spectral domain optical coherence tomography. *Br J Ophthalmol*. 2009;93:1057–1063.
27. Kim JH, Kim NR, Kim H, et al. Effect of signal strength on reproducibility of circumpapillary retinal nerve fiber layer thickness measurement and its classification by spectral-domain optical coherence tomography. *Jpn J Ophthalmol*. 2011;55:220–227.
28. Garas, A, Vargha P, Hollo G. Reproducibility of retinal nerve fiber layer and macular thickness measurement with the RTVue-100 optical coherence tomograph. *Ophthalmology*. 2010;117:738–746.
29. Paunescu LA, Schuman JS, Price LY, et al. Reproducibility of nerve fiber thickness, macular thickness, and optic nerve head measurements using StratusOCT. *Invest Ophthalmol Vis Sci*. 2004;45:1716–1724.

30. Mwanza JC, Chang RT, Budenz DL, et al. Reproducibility of peripapillary retinal nerve fiber layer thickness and optic nerve head parameters measured with cirrus HD-OCT in glaucomatous eyes. *Invest Ophthalmol Vis Sci*. 2010;51:5724–5730.
31. Budenz DL, Chang RT, Huang X, et al. Reproducibility of retinal nerve fiber thickness measurements using the stratus OCT in normal and glaucomatous eyes. *Invest Ophthalmol Vis Sci*. 2005;46:2440–2443.
32. Hong S, Kim CY, Lee WS, et al. Reproducibility of peripapillary retinal nerve fiber layer thickness with spectral domain cirrus high-definition optical coherence tomography in normal eyes. *Jpn J Ophthalmol*. 2010;54:43–47.
33. Lee SH, Kim SH, Kim TW, et al. Reproducibility of retinal nerve fiber thickness measurements using the test-retest function of spectral OCT/SLO in normal and glaucomatous eyes. *J Glaucoma*. 2010;19:637–642.
34. Savini G, Carbonelli M, Parisi V, et al. Effect of pupil dilation on retinal nerve fibre layer thickness measurements and their repeatability with Cirrus HD-OCT. *Eye (Lond)*. 2010;24:1503–1508.
35. Mansoori T, Viswanath K, Balakrishna N. Reproducibility of peripapillary retinal nerve fibre layer thickness measurements with spectral domain optical coherence tomography in normal and glaucomatous eyes. *Br J Ophthalmol*. 2011;95:685–688.
36. Nakatani Y, Higashide T, Okhubo S, et al. Evaluation of macular thickness and peripapillary retinal nerve fiber layer thickness for detection of early glaucoma using spectral domain optical coherence tomography. *J Glaucoma*. 2011;20:252–259.
37. Leung CK, Cheung CY, Weinreb RN, et al. Retinal nerve fiber layer imaging with spectral-domain optical coherence tomography: a variability and diagnostic performance study. *Ophthalmology*. 2009;116:1257–1263, 1263 e1–2.
38. Hong JT, Sung KR, Cho JW, et al. Retinal nerve fiber layer measurement variability with spectral domain optical coherence tomography. *Korean J Ophthalmol*. 2012;26:32–38.
39. Tan BB, Natividad M, Chua KC, et al. Comparison of retinal nerve fiber layer measurement between 2 spectral domain OCT instruments. *J Glaucoma*. 2012;21:266–273.
40. Czudowska MA, Ramdas WD, Wolfs RC, et al. Incidence of glaucomatous visual field loss: a ten-year follow-up from the Rotterdam study. *Ophthalmology*. 2010;117:1705–1712.